MODELING AND SIMULATION OF OVERCONSTRAINED CLOSED-LOOP MECHANISMS

Nikolay Bratovanov, Zlatko Sotirov, Vladimir Zamanov

Abstract: *The article describes an approach to modeling and motion simulation of a class of overconstrained closed-loop mechanisms. Typical behavior of overconstrained closed-loop mechanisms exhibits local mobility when near specific (singular) configurations. The mechanism's behavior in these configurations is analyzed and the direct/ inverse kinematic problems are resolved. A C++ computer program performing all the required math operations has been developed for the purpose. The verification of the computed results is done with the help of SolidWorks CAD software and a 3D model of the studied mechanism. Motion simulation is performed by using the SolidWorks application-programming interface (API).*
Keywords: *overconstrained closed-loop mechanisms, SolidWorks 3D modeling, SolidWorks API, motion simulation;*

1. Introduction

Parallel manipulators (PM) have gained significant research interest over the last 30 years [1], [3], [6], [7]. Regardless of the fact that many PM have found industrial application, the implementation of overconstrained PM (OCPM) is still limited. In 1996, Genmark Automation, Inc. developed and started to manufacture a special type of OCPM for semiconductor automation. The mechanism was named GPR™ (from "Gimbal Positioning Robot") and was trademarked and patented in 1996 [4]. The GPR mechanism had 3 DOF and was designed to perform two small independent rotations in the range of ±2 degrees and a larger-range (up to 20") translation. The terminal link (platform) was used as a basis for installing serial planar-arms (one or two) with up to 3 DOF each. The resulting hybrid parallel-serial mechanism was capable of adapting to misaligned equipment and compensating for the deflection of the manipulated object, particularly in the case of a very thin object [5]. Since 1996, thousands of GPRs have been implemented in various semiconductor FABs, turning out to be one of the largest industrial implementations of OCPM in the world. A distinctive feature of the overconstrained GPR mechanism is its performance at singular configurations – the ability to "use" the inherent elasticity and backlash of its components in order to perform the required small rotations instead of using additional kinematic joints. In the case of OCPMs, "overconstrained" does not indicate that mechanism does not move; rather, in this case, "overconstrained" indicates that the mechanism has less mobility as required by the manipulating task (i.e. it has motion deficiency in

some directions). In other words, specific moves would not exist if the mechanism was ideal, becoming possible only because of its imperfections (inherent elasticities and backlashes of components). The paper proposes how to eliminate this deficiency and provide a formal description of the motion of the mechanism. Since there are various ways of modeling the behavior of the GPR mechanism, this work attempts to explore one of the possibilities, which is considered more "natural" by the authors. It also intends to answer questions that have not yet been addressed, such as, how the platform rotations (tilting) affect its absolute positional accuracy (i.e. how the center of the platform moves as the platform rotates). In order to study the motion of the GPR mechanism the authors introduce virtual sliding joints at the platform, which represent the effect of the cumulative elasticity and backlash of the components of the mechanism.

2. Structure of the GPR™ Mechanism

The GPR mechanism consists of a base and a platform connected by three rods and kinematic joints. The three rods are parallel and are connected to the base via fifth-order sliding joints. The axes of these joints are parallel. The three rods are connected to the platform via spherical joints. The sliding joints are active and the spherical are passive. There are two orthonormal coordinate frames, $\mathrm{O}_b\mathbf{e}_{b1}\mathbf{e}_{b2}\mathbf{e}_{b3}$ and $\mathrm{O}_p\mathbf{e}_{p1}\mathbf{e}_{p2}\mathbf{e}_{p3}$, firmly attached to the base and the platform respectively. The centers of the spherical joints are denoted by $\mathrm{P}_k, k = 1,2,3$ and the intersection points of the sliding joints with the plane of the base passing through the origin O_b are denoted by $\mathrm{B}_k, k = 1,2,3$. There are also a number of radius-vectors defined: $\mathbf{r}_{O_bP_k} = (x_{O_bP_k} \;\; y_{O_bP_k} \;\; z_{O_bP_k})^T$; $\mathbf{r}_{bk} = \overrightarrow{\mathrm{O}_b\mathrm{B}_k}$; $\mathbf{r}_{pk} = \overrightarrow{\mathrm{O}_p\mathrm{P}_k}$; $= \overrightarrow{\mathrm{O}_b\mathrm{P}_k}$; $\mathbf{r}_{P_kP_l} = \overrightarrow{\mathrm{P}_k\mathrm{P}_l}$, see *Figure 1* and *Figure 2*. The length of $\overrightarrow{\mathrm{B}_k\mathrm{P}_k}$ is denoted by q_k and $\mathbf{q} = (q_1 \;\; q_2 \;\; q_3)^T$ is the vector of the generalized coordinates.

3. Mobility Analysis

The position and the orientation of all the links of the mechanism are uniquely defined by a set of parameters $\mathbf{P} \in \mathfrak{R}^N$ which are not necessarily independent. A convenient choice for $\mathbf{P}$ is $(\mathbf{q}^T \;\; \mathbf{r}_{O_bP_1}^T \;\; \mathbf{r}_{O_bP_2}^T \;\; \mathbf{r}_{O_bP_3}^T)^T$. The equations of constraints imposed on $\mathbf{P}$ by the mechanism are:

$$\mathbf{\Phi}: \mathfrak{R}^{\mathrm{N}} \to \mathfrak{R}^{\mathrm{N}}: \; \mathbf{\Phi}(\mathbf{P}) = 0 \tag{1}$$

Given the definition of $\mathbf{P}$, eq. (1). can be rewritten as

$$\begin{aligned}
\mathbf{r}_{b1} + q_1\mathbf{e}_{b3} - \mathbf{r}_{O_bP_1} &= 0 \\
\mathbf{r}_{b2} + q_2\mathbf{e}_{b3} - \mathbf{r}_{O_bP_2} &= 0 \\
\mathbf{r}_{b3} + q_3\mathbf{e}_{b3} - \mathbf{r}_{O_bP_3} &= 0 \\
(\mathbf{r}_{O_bP_2} - \mathbf{r}_{O_bP_1})^2 - L_{12}^2 &= 0 \\
(\mathbf{r}_{O_bP_3} - \mathbf{r}_{O_bP_2})^2 - L_{23}^2 &= 0 \\
(\mathbf{r}_{O_bP_1} - \mathbf{r}_{O_bP_3})^2 - L_{31}^2 &= 0
\end{aligned}$$

The Jacobian matrix of $\mathbf{\Phi}(\mathbf{P})$ is

$$\frac{d\mathbf{\Phi}}{d\mathbf{P}} = \begin{pmatrix} \mathbf{A}_{11} & -\mathbf{I}_3 & \mathbf{0}_3 & \mathbf{0}_3 \\ \mathbf{A}_{21} & \mathbf{0}_3 & -\mathbf{I}_3 & \mathbf{0}_3 \\ \mathbf{A}_{31} & \mathbf{0}_3 & \mathbf{0}_3 & -\mathbf{I}_3 \\ \mathbf{0}_3 & \mathbf{A}_{42} & \mathbf{A}_{43} & \mathbf{A}_{44} \end{pmatrix}; \quad \mathbf{A}_{11} = \begin{pmatrix} 0 & 0 & 0 \\ 0 & 0 & 0 \\ 1 & 0 & 0 \end{pmatrix}, \mathbf{A}_{21} = \begin{pmatrix} 0 & 0 & 0 \\ 0 & 0 & 0 \\ 0 & 1 & 0 \end{pmatrix}, \mathbf{A}_{31} = \begin{pmatrix} 0 & 0 & 0 \\ 0 & 0 & 0 \\ 0 & 0 & 1 \end{pmatrix}$$

$$\mathbf{A}_{42} = \begin{pmatrix} -2(x_{O_bP_2} - x_{O_bP_1}) & -2(y_{O_bP_2} - y_{O_bP_1}) & -2(z_{O_bP_2} - z_{O_bP_1}) \\ 0 & 0 & 0 \\ 2(x_{O_bP_1} - x_{O_bP_3}) & 2(y_{O_bP_1} - y_{O_bP_3}) & 2(z_{O_bP_1} - z_{O_bP_3}) \end{pmatrix}$$

$$\mathbf{A}_{43} = \begin{pmatrix} 2(x_{O_bP_2} - x_{O_bP_1}) & 2(y_{O_bP_2} - y_{O_bP_1}) & 2(z_{O_bP_2} - z_{O_bP_1}) \\ -2(x_{O_bP_3} - x_{O_bP_2}) & -2(y_{O_bP_3} - y_{O_bP_2}) & -2(z_{O_bP_3} - z_{O_bP_2}) \\ 0 & 0 & 0 \end{pmatrix}$$

$$\mathbf{A}_{44} = \begin{pmatrix} 0 & 0 & 0 \\ 2(x_{O_bP_3} - x_{O_bP_2}) & 2(y_{O_bP_3} - y_{O_bP_2}) & 2(z_{O_bP_3} - z_{O_bP_2}) \\ -2(x_{O_bP_1} - x_{O_bP_3}) & -2(y_{O_bP_1} - y_{O_bP_3}) & -2(z_{O_bP_1} - z_{O_bP_3}) \end{pmatrix}$$

The mobility of the mechanism characterized by its DOF is $h = N - Rank\left(\frac{d\mathbf{\Phi}}{d\mathbf{P}}\right)$ [2]. In the case of $q_1 = q_2 = q_3$, $Rank\left(\frac{d\mathbf{\Phi}}{d\mathbf{P}}\right) = 9$ and $h = 3$. In other words, the platform has instantaneous local mobility with dimension 3. Even small differences in the coordinates q_1, q_2, q_3, which are in the range of the normal deviations from the parallelism of the rods connecting the platform to the base, brings $Rank\left(\frac{d\mathbf{\Phi}}{d\mathbf{P}}\right)$ to 11. This means that the platform has a single DOF at the specific configuration, which is an apparent deficiency. The GPR mechanism is designed to work in a close vicinity of the singular configuration $q_1 = q_2 = q_3$. It has to perform two small (±1.5 deg) independent rotations of the platform about an axis which lies in the plane of the platform and a vertical translation in a larger-range. Since $Rank\left(\frac{d\mathbf{\Phi}}{d\mathbf{P}}\right)$ is equal to 11 everywhere except for $q_1 = q_2 = q_3$, the constraints imposed to the platform by the spherical joints has to be relieved. In real, this happens naturally because of the imperfection of the joints and the inherent elasticity of the links, which compensates the 2 DOF deficiency. To model this behavior, we introduce three virtual sliding joints at the platform as shown in *Figure 1*. The axes of these joints coincide with the respective radius-vectors $\overrightarrow{O_pP_k}$. The geometry of the GPR mechanism can be represented by the following parameters $\mathbf{X} = (l_1 \ l_2 \ l_3)^T$ and $\mathbf{Y} = (L_{12} \ L_{23} \ L_{31})^T$. At singular configuration $l_1 = l_2 = l_3$ and $L_{12} = L_{23} = L_{31}$, see *Figure 3a*. *Figure 3b* shows a configuration with tilted platform $l_1 \neq l_2 \neq l_3$ and $L_{12} \neq L_{23} \neq L_{31}$. As it is seen from this figure, the center of the platform is shifted in the amount of $d\mathbf{r}$ as a result of the tilting. In order to solve the direct and the inverse kinematic problems the equations of constraints imposed on $\mathbf{X}$ and $\mathbf{Y}$ and their derivatives have to be studied. The following expressions characterize the relationship between $\mathbf{X}$, $\mathbf{Y}$, $\dot{\mathbf{X}}$ and $\dot{\mathbf{Y}}$:

$$\mathbf{F}(\mathbf{X}, \mathbf{Y}) = \mathbf{0}, \tag{2}$$

which is the same as

$$l_1^2 + l_2^2 + l_1 l_2 - L_{12}^2 = 0$$
$$l_2^2 + l_3^2 + l_2 l_3 - L_{23}^2 = 0$$
$$l_3^2 + l_1^2 + l_3 l_1 - L_{31}^2 = 0$$

$$\frac{\partial \mathbf{F}}{\partial \mathbf{X}} = \begin{pmatrix} 2l_1 + l_2 & 2l_2 + l_1 & 0 \\ 0 & 2l_2 + l_3 & 2l_3 + l_2 \\ 2l_1 + l_3 & 0 & 2l_3 + l_1 \end{pmatrix}$$

$$\frac{\partial \mathbf{F}}{\partial \mathbf{Y}} = \begin{pmatrix} -2L_{12} & 0 & 0 \\ 0 & -2L_{23} & 0 \\ 0 & 0 & -2L_{31} \end{pmatrix}$$

$$\frac{\partial \mathbf{F}}{\partial \mathbf{X}}\dot{\mathbf{X}} + \frac{\partial \mathbf{F}}{\partial \mathbf{Y}}\dot{\mathbf{Y}} = \mathbf{0} \tag{3}$$

$$\dot{\mathbf{X}} = -\left(\frac{\partial \mathbf{F}}{\partial \mathbf{X}}\right)^{-1} \frac{\partial \mathbf{F}}{\partial \mathbf{Y}}\dot{\mathbf{Y}} = \frac{\partial \mathbf{X}}{\partial \mathbf{Y}}\dot{\mathbf{Y}} \tag{4}$$

$$\dot{\mathbf{Y}} = -\left(\frac{\partial \mathbf{F}}{\partial \mathbf{Y}}\right)^{-1} \frac{\partial \mathbf{F}}{\partial \mathbf{X}}\dot{\mathbf{X}} = \frac{\partial \mathbf{Y}}{\partial \mathbf{X}}\dot{\mathbf{X}} \tag{5}$$

Solving eq. (2) for **X** is not straightforward, requiring the use of the well-known Newton-Euler iterative approach. The solutions for $\dot{\mathbf{X}}$ and $\dot{\mathbf{Y}}$ are explicit and require conventional matrix-operations, including matrix-inversion, see eq. (4) and eq. (5).

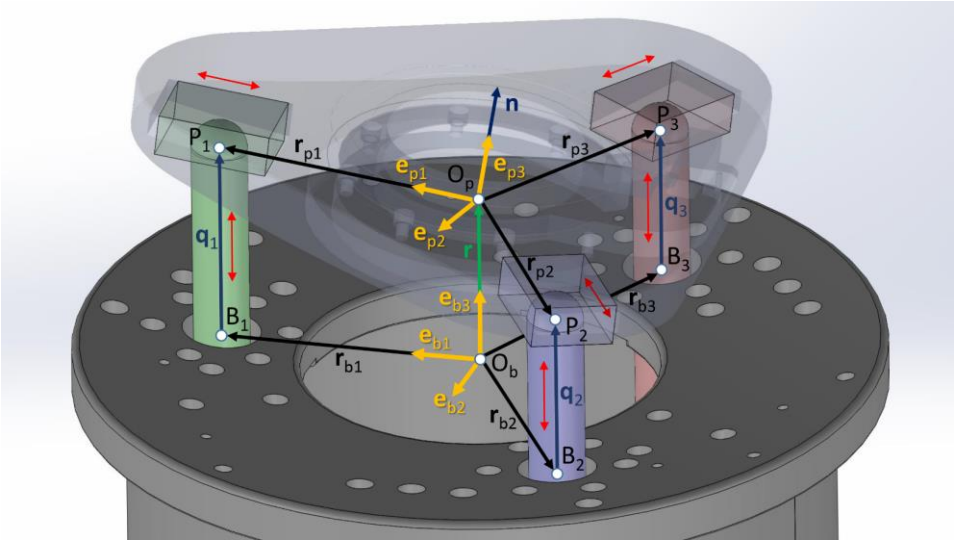

Figure 1. GPR mechanism geometry.

4. Direct Kinematics

Given the generalized coordinates $\mathbf{q} = (q_1\ q_2\ q_3)^T$ find the radius-vector **r** of the center of the platform O_p with respect to the center of the base O_b and the orientation of the platform represented by its normal vector **n,** which coincides with $\mathbf{e}_{p3}$. The first step of the direct kinematics solution is to solve eq. (2) for **X,** given $\mathbf{Y}_d$. The radius-vectors of the center of the spherical joints at the platform with respect to the cen-

ter of the base are $\mathbf{r}_{O_bP_1} = \mathbf{r}_{b1} + q_1\mathbf{e}_{b3}$, $\mathbf{r}_{O_bP_2} = \mathbf{r}_{b2} + q_2\mathbf{e}_{b3}$ and $\mathbf{r}_{O_bP_3} = \mathbf{r}_{b3} + q_3\mathbf{e}_{b3}$. The last define the vectors between the centers of the spherical joints at the platform $\mathbf{r}_{P_1P_2} = \mathbf{r}_{O_bP_2} - \mathbf{r}_{O_bP_1}$, $\mathbf{r}_{P_2P_3} = \mathbf{r}_{O_bP_3} - \mathbf{r}_{O_bP_2}$ and $\mathbf{r}_{P_3P_1} = \mathbf{r}_{O_bP_3} - \mathbf{r}_{O_bP_1}$. The components of the desired vector $\mathbf{Y}$ are the Euclidean norms of $\mathbf{r}_{P_1P_2}$, $\mathbf{r}_{P_2P_3}$ and $\mathbf{r}_{P_3P_1}$, which in turn represent the lengths L_{12}, L_{23} and L_{31} respectively:

$$\mathbf{Y}_d = (\|\mathbf{r}_{P_1P_2}\| \; \|\mathbf{r}_{P_2P_3}\| \; \|\mathbf{r}_{P_3P_1}\|)^T$$

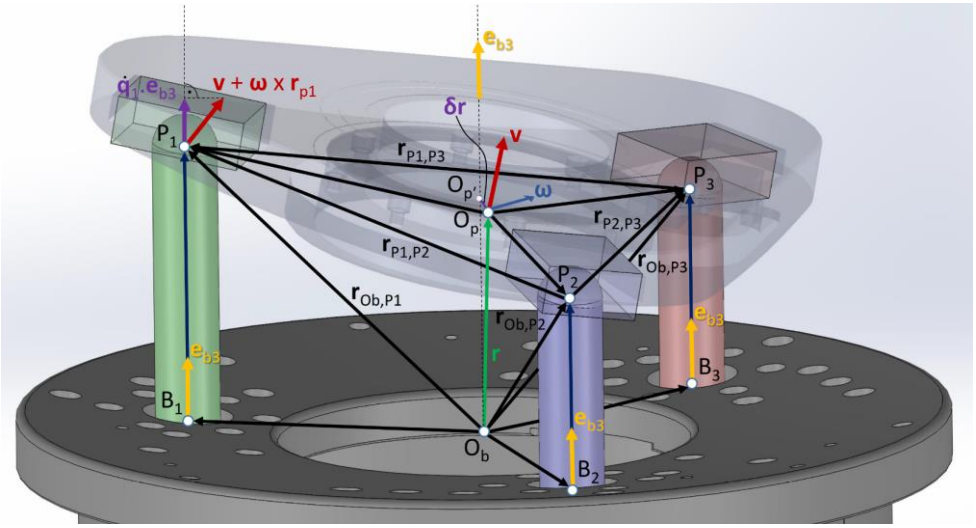

Figure 2. GPR Velocity Distribution.

The initial value of $\mathbf{X}$ corresponds to $q_1 = q_2 = q_3$, i.e. $\mathbf{X}_0 = (R \;\; R \;\; R)^T$, where $R = |O_pP_1| = |O_pP_2| = |O_pP_3|$ is the radius of the platform. The initial value of $\mathbf{Y}$ is $\mathbf{Y}_0 = \left(R\sqrt{3} \;\; R\sqrt{3} \;\; R\sqrt{3}\right)^T$. Given $\mathbf{Y}_\mathrm{d}$, $\mathbf{X}_0$ and $\mathbf{Y}_0$, the value of $\mathbf{X}$ which corresponds to $\mathbf{Y}_\mathrm{d}$ is determined via the well-known Newton-Rapson iterative procedure:

$$\mathbf{X}_k = \mathbf{X}_{k-1} + \frac{\partial \mathbf{X}}{\partial \mathbf{Y}}(\mathbf{Y}_d - \mathbf{Y}_{k-1}) \qquad k = 1, 2\ldots$$

Normally, it takes 2-3 iterations to find a very accurate solution to the equation $\mathbf{X}_d = \mathbf{X}(\mathbf{Y}_d)$. Once $\mathbf{X}_d$ is found, the calculation of the radius-vector $\mathbf{r}$ of the center of the platform w.r.t. the center of the base and the orientation of the platform becomes straightforward. The unit normal-vector of the platform is calculated as

$$\mathbf{n} = (\mathbf{r}_{P_1P_2} \times \mathbf{r}_{P_2P_3})/\|\mathbf{r}_{P_1P_2} \times \mathbf{r}_{P_2P_3}\|$$

and the radius-vector $\mathbf{r}$ as

$$\mathbf{r} = \mathbf{r}_{b1} + q_1\mathbf{e}_3 + l_1\, cos(\delta)\, \mathbf{e}_{P_1P_2} + l_1\, sin(\delta)\, (\mathbf{n} \times \mathbf{e}_{P_1P_2}) \tag{6}$$

where

$$\mathbf{e}_{P_1P_2} = \frac{\mathbf{r}_{P_1P_2}}{\|\mathbf{r}_{P_1P_2}\|};\;\; cos(\delta) = \frac{l_1^2 - l_2^2 + L_{12}^2}{2l_1L_{12}};\;\; sin(\delta) = \sqrt{1 - cos^2(\delta)}$$

5. Inverse Kinematics

5.1. Position

Given the position of the platform z$\mathbf{e}_3$, where $\mathbf{e}_3 = (0\ \ 0\ \ 1)^T$ and its normal vector $\mathbf{n}_d$ find the length of the rods $\mathbf{q} = (q_1\ q_2\ q_3)^T$ connecting the base and the platform. The desired normal vector of the platform $\mathbf{n}_d$ can be obtained by rotating the unit vector $\mathbf{e}_3$ about $\mathbf{e}_1 = (1\ 0\ 0)$ by an angle α and then rotating the resulting vector $\mathbf{n}_\alpha$ about $\mathbf{e}_2 = (0\ 1\ 0)$ by an angle β.

$$\mathbf{n}_\alpha = \mathbf{n}_3 \cos(\alpha) + (\mathbf{e}_1 \times \mathbf{n}_3)\sin(\alpha) + \mathbf{e}_1(\mathbf{e}_1.\mathbf{n}_3)(1-\cos(\alpha))$$
$$\mathbf{n}_d = \mathbf{n}_{\alpha\beta} = \mathbf{n}_\alpha \cos(\beta) + (\mathbf{e}_2 \times \mathbf{n}_\alpha)\sin(\beta) + \mathbf{e}_2(\mathbf{e}_2.\mathbf{n}_\alpha)(1-\cos(\beta))$$

Then the vector of the generalized coordinates can be determined as

$$\mathbf{q} = \begin{pmatrix} \dfrac{(z\mathbf{e}_{b3} - \mathbf{r}_{b1}).\mathbf{n}_d}{\mathbf{e}_{b3}.\mathbf{n}_d} \\ \dfrac{(z\mathbf{e}_{b3} - \mathbf{r}_{b2}).\mathbf{n}_d}{\mathbf{e}_{b3}.\mathbf{n}_d} \\ \dfrac{(z\mathbf{e}_{b3} - \mathbf{r}_{b3}).\mathbf{n}_d}{\mathbf{e}_{b3}.\mathbf{n}_d} \end{pmatrix} \tag{7}$$

Note that due to the overconstrained nature of the GPR mechanism, the center of the platform may slightly shift with respect to z$\mathbf{e}_3$. Therefore, once the generalized coordinates according to eq. (7) are found, the actual position of the center of the platform must be calculated through the solution to the direct kinematics problem, see Section 1.

5.2. Velocity

Given $\mathbf{v} = (0\ 0\ \dot{z}\mathbf{e}_{b3})^T$ and $\boldsymbol{\omega} = (\omega_1\ \omega_2\ 0)^T$ find $\dot{\mathbf{q}}$ and $\dot{\mathbf{r}}$. The desired angular velocity can be defined as $\boldsymbol{\omega} = \dot{\alpha}\mathbf{v}$, where $\mathbf{v} = \cos(\beta)\,\mathbf{e}_{p1} + \sin(\beta)\,\mathbf{e}_{p2}$, $\mathbf{e}_{p1} = \mathbf{r}_{O_pP_1} / \left\|\mathbf{r}_{O_pP_1}\right\|$ and $\mathbf{e}_{p2} = \mathbf{n} \times \mathbf{e}_{p1}$. The vector of the generalized velocities can be determined by projecting the velocities of the points P_1, P_2 and P_3 onto $\mathbf{e}_{b3}$, see Figure 3:

$$\dot{\mathbf{q}} = \begin{pmatrix} \mathbf{e}_{b3}.(\mathbf{v} + \boldsymbol{\omega} \times \mathbf{r}_{p_1}) \\ \mathbf{e}_{b3}.(\mathbf{v} + \boldsymbol{\omega} \times \mathbf{r}_{p_2}) \\ \mathbf{e}_{b3}.(\mathbf{v} + \boldsymbol{\omega} \times \mathbf{r}_{p_3}) \end{pmatrix} \tag{8}$$

The velocity of the center of the platform is determined by differentiating eq. (6):

$$\dot{\mathbf{r}} = \dot{q}_1\mathbf{e}_{b3} + \left[\dot{l}_1\, cos(\delta) - l_1\, sin(\delta)\dot{\delta}\right]\mathbf{e}_{P_1P_2} + l_1\, cos(\delta)\left(\boldsymbol{\omega} \times \mathbf{e}_{P_1P_2}\right) +$$
$$\left[\dot{l}_1\, sin(\delta) + l_1 cos(\delta)\dot{\delta}\right]\left(\mathbf{n} \times \mathbf{e}_{P_1P_2}\right) + l_1\, sin(\delta)\left[(\boldsymbol{\omega} \times \mathbf{n}) \times \mathbf{e}_{P_1P_2} + \mathbf{n} \times \left(\boldsymbol{\omega} \times \mathbf{e}_{P_1P_2}\right)\right] \tag{9}$$

by taking into consideration that $\dot{\mathbf{n}} = \boldsymbol{\omega} \times \mathbf{n}$, $\mathbf{e}_{P_1P_2} = \mathbf{r}_{P_1P_2} / \left\| \mathbf{r}_{P_1P_2} \right\|$ and

$$\dot{\delta} = \frac{2\left(l_1\dot{l}_1 - l_2\dot{l}_2 + L_{12}\dot{L}_{12}\right)l_1L_{12} + (l_2^2 - l_1^2 - L_{12}^2)(\dot{l}_1L_{12} + l_1\dot{L}_{12})}{2l_1L_{12}^2\, sin(\delta)}.$$

The values of $\dot{l}_1$ and $\dot{l}_2$ are derived from eq. (4) given $\dot{\mathbf{Y}} = \left((\dot{q}_2 - \dot{q}_1)\mathbf{e}_{b3} \;\; (\dot{q}_3 - \dot{q}_2)\mathbf{e}_{b3} \;\; (\dot{q}_3 - \dot{q}_1)\mathbf{e}_{b3}\right)^T$.

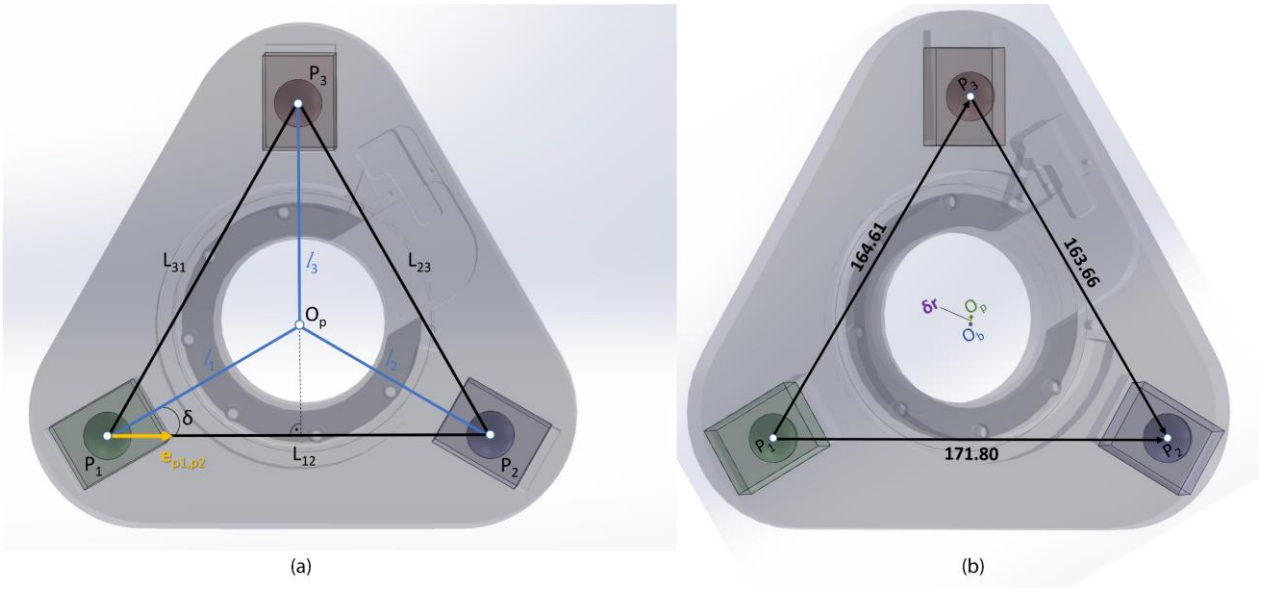

Figure 3. Platform geometry. (a) – parallel to the base; (b) – tilted.

5.3. Acceleration

Given $\dot{\mathbf{v}} = (0\ 0\ \ddot{z}\mathbf{e}_{b3})^T$, $\boldsymbol{\omega} = (\omega_1\ \omega_2\ 0)^T$ and $\dot{\boldsymbol{\omega}} = (\dot{\omega}_1\ \dot{\omega}_2\ 0)^T$ find $\ddot{\mathbf{q}}$ and $\ddot{\mathbf{r}}$. The vector of the generalized acceleration can be obtained by differentiating eq. (8)

$$\ddot{\mathbf{q}} = \begin{pmatrix} \mathbf{e}_{b3}.\left[\dot{\mathbf{v}} + \dot{\boldsymbol{\omega}} \times \mathbf{r}_{p_1} + \boldsymbol{\omega} \times (\boldsymbol{\omega} \times \mathbf{r}_{p_1})\right] \\ \mathbf{e}_{b3}.\left[\dot{\mathbf{v}} + \dot{\boldsymbol{\omega}} \times \mathbf{r}_{p_2} + \boldsymbol{\omega} \times (\boldsymbol{\omega} \times \mathbf{r}_{p_2})\right] \\ \mathbf{e}_{b3}.\left[\dot{\mathbf{v}} + \dot{\boldsymbol{\omega}} \times \mathbf{r}_{p_3} + \boldsymbol{\omega} \times (\boldsymbol{\omega} \times \mathbf{r}_{p_3})\right] \end{pmatrix}$$

The calculation of the acceleration of the center of the platform requires availability of $\ddot{\mathbf{X}}$. The last can be determined by differentiating eq. (3) and solving for $\ddot{\mathbf{X}}$:

$$\ddot{\mathbf{X}} = -\left(\frac{\partial \mathbf{F}}{\partial \mathbf{X}}\right)^{-1}\left[\frac{d}{dt}\left(\frac{\partial \mathbf{F}}{\partial \mathbf{X}}\right)\dot{\mathbf{X}} + \frac{d}{dt}\left(\frac{\partial \mathbf{F}}{\partial \mathbf{Y}}\right)\dot{\mathbf{Y}} + \frac{\partial \mathbf{F}}{\partial \mathbf{Y}}\ddot{\mathbf{Y}}\right]$$

The vector $\ddot{\boldsymbol{Y}}$ and the matrices $\frac{d}{dt}\left(\frac{\partial \boldsymbol{F}}{\partial \boldsymbol{X}}\right)$ and $\frac{d}{dt}\left(\frac{\partial \boldsymbol{F}}{\partial \boldsymbol{Y}}\right)$ are calculated as follows:

$$\ddot{\mathbf{Y}} = ((\ddot{q}_2 - \ddot{q}_1)\ \mathbf{e}_{b3} \;\; (\ddot{q}_3 - \ddot{q}_2)\mathbf{e}_{b3} \;\; (\ddot{q}_3 - \ddot{q}_1)\mathbf{e}_{b3})^T$$

$$\frac{d}{dt}\left(\frac{\partial \mathbf{F}}{\partial \mathbf{X}}\right) = \begin{pmatrix} 2\dot{l}_1 + \dot{l}_2 & 2\dot{l}_2 + \dot{l}_1 & 0 \\ 0 & 2\dot{l}_2 + \dot{l}_3 & 2\dot{l}_3 + \dot{l}_2 \\ 2\dot{l}_1 + \dot{l}_3 & 0 & 2\dot{l}_3 + \dot{l}_1 \end{pmatrix}; \quad \frac{d}{dt}\left(\frac{\partial \mathbf{F}}{\partial \mathbf{Y}}\right) = \begin{pmatrix} -2\dot{L}_{12} & 0 & 0 \\ 0 & -2\dot{L}_{23} & 0 \\ 0 & 0 & -2\dot{L}_{31} \end{pmatrix}$$

Finally, $\ddot{\mathbf{r}}$ is obtained by differentiating eq. (9)

$$\begin{aligned}\ddot{\mathbf{r}} = {} & \ddot{q}_1\mathbf{e}_{b3} + \left[\ddot{l}_1\cos(\delta) - 2\dot{l}_1\sin(\delta)\dot{\delta} - l_1\cos(\delta)\dot{\delta}^2 - l_1\sin(\delta)\ddot{\delta}\right]\mathbf{e}_{P_1P_2} \\ & + \left[l_1\cos(\delta) - l_1\sin(\delta)\dot{\delta}\right](\boldsymbol{\omega}\times\mathbf{e}_{P_1P_2}) + \left[\dot{l}_1\cos(\delta) - l_1\sin(\delta)\dot{\delta}\right](\boldsymbol{\omega}\times\mathbf{e}_{P_1P_2}) \\ & + l_1\cos(\delta)\left\{(\dot{\boldsymbol{\omega}}\times\mathbf{e}_{P_1P_2}) + \left[\boldsymbol{\omega}\times(\boldsymbol{\omega}\times\mathbf{e}_{P_1P_2})\right]\right\} \\ & + \left[\ddot{l}_1\sin(\delta) + 2\dot{l}_1\sin(\delta)\dot{\delta} - l_1\sin(\delta)\dot{\delta}^2 - l_1\cos(\delta)\ddot{\delta}\right](\mathbf{n}\times\mathbf{e}_{P_1P_2}) \\ & + \left[l_1\sin(\delta) + l_1\cos(\delta)\dot{\delta}\right]\left[(\boldsymbol{\omega}\times\mathbf{n})\times\mathbf{e}_{P_1P_2} + \mathbf{n}\times(\boldsymbol{\omega}\times\mathbf{e}_{P_1P_2})\right] \\ & + l_1\sin(\delta)\left\{[\boldsymbol{\omega}\times\mathbf{n} + \boldsymbol{\omega}\times(\boldsymbol{\omega}\times\mathbf{n})]\times\mathbf{e}_{P_1P_2} + 2(\boldsymbol{\omega}\times\mathbf{n})\times(\boldsymbol{\omega}\times\mathbf{e}_{P_1P_2}) + \mathbf{n}\right. \\ & \left.\times\left[\dot{\boldsymbol{\omega}}\times\mathbf{e}_{P_1P_2} + \boldsymbol{\omega}\times(\boldsymbol{\omega}\times\mathbf{e}_{P_1P_2})\right]\right\}\end{aligned}$$

6. Simulations

The validity of the proposed approach to modeling the GPR mechanism was verified via computer simulations and 3D modeling with SolidWorks (API). The main goal of the simulations was to quantify the motion of the virtual sliding joints and the motion of the center of the platform corresponding to rotations of the platform in the range $[-2^o,\ 2^o]$. Figure 5 shows the displacement d$\mathbf{r}$ of the center of the platform in the direction of the unit-vectors $\mathbf{e}_{p1}\mathbf{e}_{p2}\mathbf{e}_{p3}$, denoted by dx, dy and dz, respectively. As it is seen from the plot, dx and dy have magnitude of less than 30 micron. The deviation in the vertical direction dz is negligibly small (less than 2 micron).

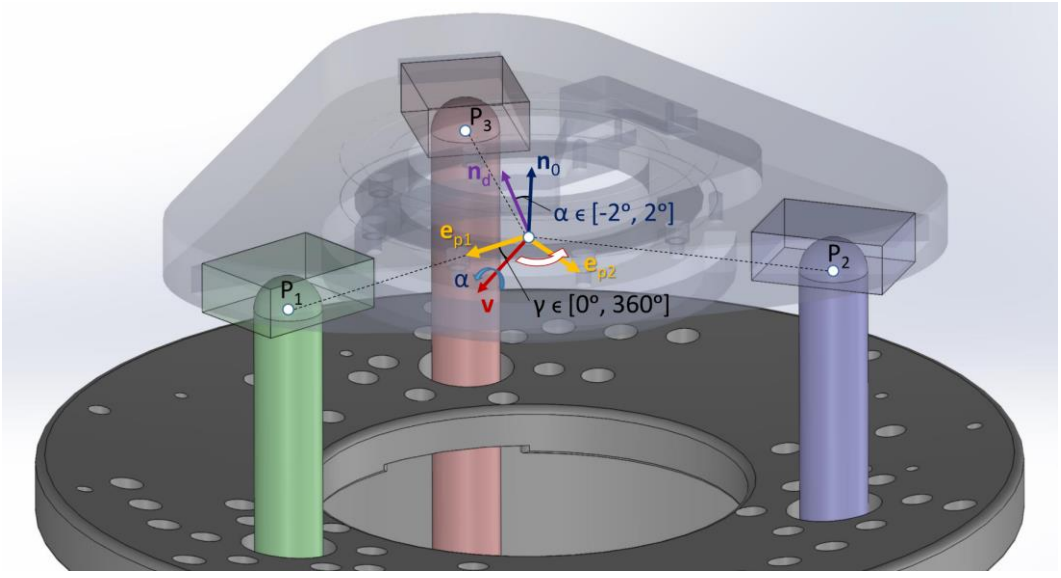

Figure 4. Simulation scenario (vector and angle of rotation of the platform).

At singularity $l_1 = l_2 = l_3 = 93.224$ mm. As the platform rotates in the range $[-2^o,\ 2^o]$, the maximum absolute deviation of $l_1,\ l_2$ and l_3 from 93.224 mm is less than 80 micron, see Figure 6. Therefore, if the cumulative contribution of the backlash and the elasticity associated with the components (spherical bearings and rods) con-

necting the platform and the base allow for 60 micron deviation of the center of the spherical joints from their ideal position, the platform will be able to tilt in the range $[-2^o,\ 2^o]$. Figure 7, shows how dx and dy change as the platform rotates about an arbitrary vector **v** in the plane of the platform**.**

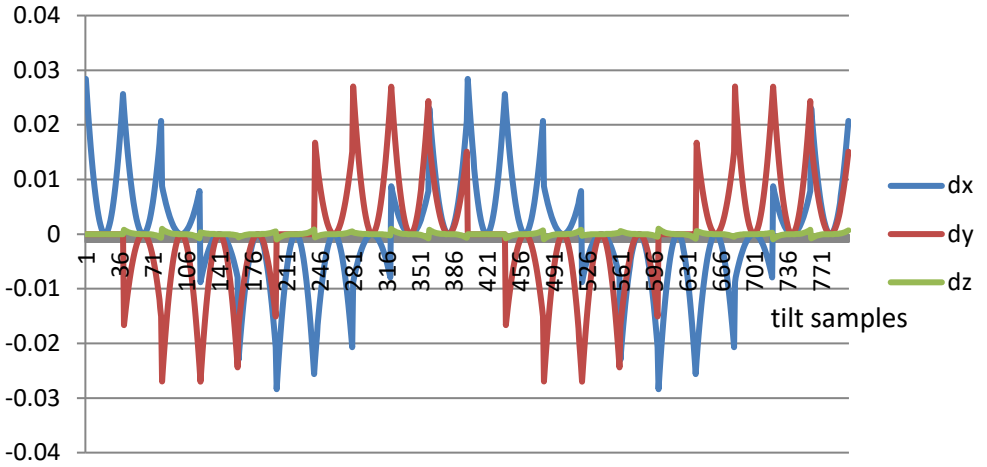

Figure 5. Deviations of the center of the platform during tilting within the whole working envelope

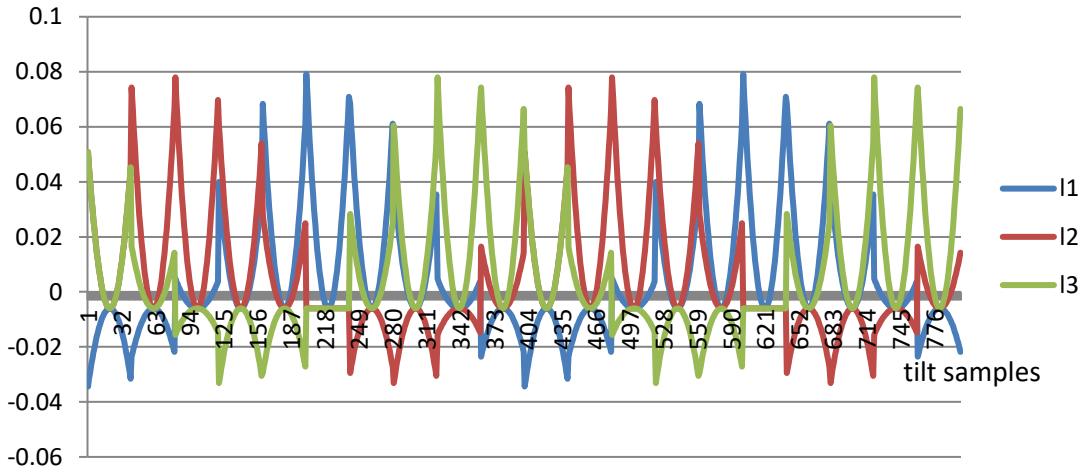

Figure 6. Motion of the virtual sliding joints during platform rotation.

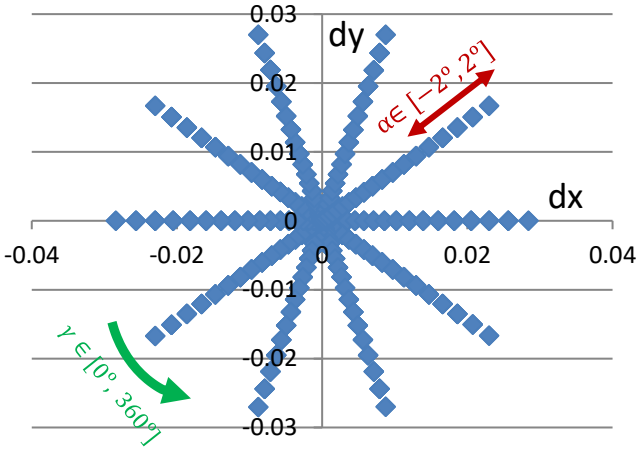

Figure 7. Deviations of the center of the platform during tilting within the whole working envelope, x-y section.

7. Conclusions

This work is the first attempt to analytically describe the principle of operation of the GPR OC mechanism. It derived the relationship between the finite rotations of the platform and the imperfections of the components connecting the platform and the base. The introduction of virtual sliding joints proved to be an effective approach to studying the kinematics of overconstrained PM in order to determine the mechanism of the small rotations in a vicinity of singular configuration. It was shown that because of the overconstrained nature of the mechanism, the center of the platform moves w.r.t. its ideal position as the platform rotates. The magnitude of this motion was calculated, proving to be very small and within the range of the inherent imperfections of the mechanism's components. The authors acknowledge that there are many different ways for introducing virtual joints and therefore the results obtained in this study are not exhaustive. It is believed that the recent work establishes a basis for future studies in the area of kinematics and dynamics of OCPM.

References

[1] Özgün Selvi, "Structural and kinematic synthesis of overconstrained mechanisms," Ph.D. Thesis, Izmir, 2012

[2] Jian S. Dai, Zhen Huang and Harvey Lipkin, "Mobility of Overconstrained Parallel Mechanisms," J. Mech. Des 128(1), 220-229 (Oct 14, 2004)

[3] Grigore GOGU, "Structural and Kinematic Structural and Kinematic Analysis and Synthesis of Analysis and Synthesis of Parallel Robot," SSIR-Clermont-Ferrand - June 27, 2008

[4] Genov, G., Todorov, D., "Universally Tiltable Z-Axis Drive", US Patent US5954840, June 13, 1996

[5] Genov, G., Sotirov, Z., and Bonev, E., "Robot Motion Compensation System", US Patent US6489741B1, August 1998

[6] Sheng Guo, Haibo Qu, Yuefa Fang, Congzhe Wang, "The DOF Degeneration Characteristics of Closed-Loop Overconstrained Mechanisms, Transactions of the Canadian Society for Mechanical Engineering, Vol. 36, No. 1, 2012

[7] Sotirov, Z.M., "Parallel-Series Manipulators in Semiconductor Automation "Semiconductor European, July 2002

Authors: Nikolay Bratovanov, PhD student, "Robotics Research Laboratory", Technical University of Sofia, e-mail: nbratovanov@gmail.com; Zlatko Sotirov, PhD, Executive Vice President of Engineering and Chief Scientist, Genmark Automation, Inc., e-mail: zsotirov@genmarkautomation.com; Vladimir Zamanov, Associate Professor, PhD, Faculty of Automatics, Technical University of Sofia, e-mail: vzamanov@tu-sofia.bg